Tailoring optical metamaterials to tune the atom-surface Casimir-Polder interaction

Chan, Eng Aik; Aljunid, Syed Abdullah; Adamo, Giorgio; Laliotis, Athanasios; Ducloy, Martial; Wilkowski, David

2018

Chan, E. A., Aljunid, S. A., Adamo, G., Laliotis, A., Ducloy, M., & Wilkowski, D. (2018). Tailoring optical metamaterials to tune the atom-surface Casimir-Polder interaction. Science Advances, 4(2), eaao4223-.

https://hdl.handle.net/10356/85581

https://doi.org/10.1126/sciadv.aao4223

PHYSICS

Tailoring optical metamaterials to tune the atom-surface Casimir-Polder interaction

Eng Aik Chan,[1,2] Syed Abdullah Aljunid,[1] Giorgio Adamo,[1] Athanasios Laliotis,[3] Martial Ducloy,[1,2,3]* David Wilkowski[1,4,5,2]*

Metamaterials are fascinating tools that can structure not only surface plasmons and electromagnetic waves but also electromagnetic vacuum fluctuations. The possibility of shaping the quantum vacuum is a powerful concept that ultimately allows engineering the interaction between macroscopic surfaces and quantum emitters such as atoms, molecules, or quantum dots. The long-range atom-surface interaction, known as Casimir-Polder interaction, is of fundamental importance in quantum electrodynamics but also attracts a significant interest for platforms that interface atoms with nanophotonic devices. We perform a spectroscopic selective reflection measurement of the Casimir-Polder interaction between a Cs($6P_{3/2}$) atom and a nanostructured metallic planar metamaterial. We show that by engineering the near-field plasmonic resonances of the metamaterial, we can successfully tune the Casimir-Polder interaction, demonstrating both a strong enhancement and reduction with respect to its nonresonant value. We also show an enhancement of the atomic spontaneous emission rate due to its coupling with the evanescent modes of the nanostructure. Probing excited-state atoms next to nontrivial tailored surfaces is a rigorous test of quantum electrodynamics. Engineering Casimir-Polder interactions represents a significant step toward atom trapping in the extreme near field, possibly without the use of external fields.

INTRODUCTION

Material boundaries modify the surrounding quantum vacuum giving rise to interactions between classical macroscopic surfaces (Casimir effect) or between a surface and a quantum polarizable object (Casimir-Polder interaction) (*1*). The surface, which induces a shift of atomic energy levels, was investigated experimentally with thermal vapors (*2*–*4*), atomic beams (*5*, *6*), and cold atoms (*7*–*9*). The dispersive energy shift goes hand in hand with a dissipative change of the atomic radiative properties, allowing for the tuning of spontaneous emission rates of atoms next to dielectric surfaces. For this purpose, placing atoms next to tailored nanostructures is becoming a new challenge in the field of nanophotonics. Hybridization of atomic and nanophotonic systems paves the way to novel quantum devices due to strong atom-light coupling with microcavities (*10*) or due to collective effects arising from strong confinement (*11*, *12*). The most common hybrid platforms include tapered nanofibers (*13*), hollow core fibers (*14*), or photonic bandgap waveguides (*15*).

The Casimir-Polder force has been largely perceived as an obstacle for placing atoms close to surfaces. Nevertheless, ambitious proposals emerge that suggest the possibility of using atom-surface interactions to achieve tight trapping at record distances from surfaces (*16*) and, in particular, photonic bandgap waveguides (*17*, *18*). The tantalizing possibility of subwavelength atom trapping is made more difficult because of the predominantly attractive nature of the Casimir-Polder interaction that does not allow stable trapping potentials in all directions. Experimental demonstration of an efficient tuning of the atom-surface interaction, particularly between attraction and repulsion, represents therefore a milestone in the field of hybrid systems.

[1]Centre for Disruptive Photonic Technologies, The Photonics Institute, Nanyang Technological University (NTU), Singapore 637371, Singapore. [2]School of Physical and Mathematical Sciences, NTU, Singapore 637371, Singapore. [3]Laboratoire de Physique des Lasers, UMR 7538 du CNRS, Université Paris 13-Sorbonne Paris Cité, F-93430 Villetaneuse, France. [4]Centre for Quantum Technologies, National University of Singapore (NUS), Singapore 117543, Singapore. [5]MajuLab, CNRS–Université Nice Sophia Antipolis–NUS-NTU, Université Côte d'Azur, International Joint Research Unit, UMI 3654, Singapore, Singapore.
*Corresponding author. Email: david.wilkowski@ntu.edu.sg (D.W.); martial.ducloy@univ-paris13.fr (M.D.)

Among the various approaches to modify the Casimir-Polder interaction, one relies on the resonant coupling between excited atoms and surface resonances. Thus, experiments with cesium atoms in high-lying excited states next to a sapphire surface have demonstrated resonant Casimir-Polder repulsion (*19*, *20*) or an exaltation of the Casimir-Polder attraction with temperature (*21*). The key parameter here, which governs both strength and sign of the Casimir-Polder interaction, is the relative detuning of the surface resonance frequency compared to the predominant atomic dipole coupling (transition). Active engineering of the atom-surface interaction is therefore severely limited by the selection of dielectrics that are available in nature. The possibility of exploring material birefringence as a means of tuning the polariton resonances has been proposed (*22*), but the theoretical tunability is restricted and yet to be demonstrated experimentally.

An alternative solution would be to use nanostructured periodic planar metamaterials that allow a broad tunability of plasmonic surface resonances across the visible and near infrared spectrum. This spectral domain, where plasmonic or polaritonic resonances are usually scarce in bulk material, is of particular interest because it matches with low-lying transitions of alkali atoms, routinely used in laser cooling or atomic spectroscopy experiments. Moreover, thin metallic planar metamaterials have enhanced light transmission at the plasmon resonance. It thus becomes possible to perform reflection spectroscopy on a vapor/metamaterial interface. Previous experiments on cesium vapor demonstrated a modification of the surface reflectivity; however, analysis of the Doppler broadened spectra did not provide quantitative information on the frequency shift or the atomic lifetime modification at the proximity of the metamaterials (*23*, *24*).

Here, we report on high-resolution frequency-modulated selective reflection (SR) spectroscopy of Cs($6P_{3/2}$) atoms in vicinity of a wide range of metallic planar metamaterials. The theoretical treatment of SR on flat dielectric surfaces (*25*) is here further developed, allowing us to measure the dispersive Casimir-Polder shift of the $6S_{1/2}\leftrightarrow 6P_{3/2}$, cesium D2 transition as well as a dissipative modification of the spontaneous emission rate (*26*). For an adequately chosen metamaterial, the frequency shift on the cesium transition, induced by the Casimir-Polder

interaction, can be almost suppressed. A quantum electrodynamics (QED) calculation of the fully retarded Casimir-Polder interaction is shown to reproduce the basic features of our experimental data.

RESULTS

The system under investigation, similar to the one used by Aljunid *et al.* (*24*), is depicted in Fig. 1A. A cesium vapor at $T = 80°C$ is introduced into a vacuum chamber. The density of the atoms is around $N = 10^{17}$ m^{-3}, whereas the thermal velocity is $\bar{u} = 150$ ms^{-1}. On one of the dielectric viewports of the vacuum chamber, 10 different metamaterials are engraved on a 50-nm-thick silver layer (see Fig. 1B). Each metamaterial consists of an area of 200 μm × 200 μm containing arrays of 70-nm-wide nanoslits of varying length from 170 to 240 nm. The unit cells are squares with sizes from $w = 380$ to 520 nm long, depending on the length of the slit. We achieve plasmonic resonances, characterized by their central position, covering a wavelength range from 670 to 980 nm. Each plasmon resonance has a typical width of 60 nm (see example in Fig. 1C). The atom/metamaterial hybrid system is excited and probed on the $6S_{1/2} \leftrightarrow 6P_{3/2}$ cesium D2 transition at 852 nm, using an SR optical setup at normal incidence (*2*, *27*, *28*).

The radiation is produced by an external cavity diode laser (ECDL). Part of the light is sent to a saturated absorption spectroscopy setup used as a frequency reference. The main beam goes through an electro-optic modulator to modulate its phase at $\Omega_m = 9$ MHz with a modulation index of $\beta = 0.19$ and is then shaped by a square mask to optimize its overlap with the metamaterial. The intensity of the laser is maintained below saturation, typically $I = 1$ mW/cm^2. The reflected light beam is collected on a fast and sensitive amplified photodetector. The signal at 9 MHz is demodulated using a lock-in amplifier, directly providing the in-phase and in-quadrature component of the reflection signal, which is purely Doppler-free and analyzed in the following.

First, we analyze the reflectance and transmittance of the metamaterials at 852 nm using the ECDL. To do so, we detuned the laser away from the cesium resonance such that it is not coupled anymore to the atomic vapor, whereas the coupling to the plasmon remains unchanged. The results are summarized in Fig. 2. Here, each pair of reflectance/transmittance data corresponds to a given metamaterial, which is characterized by its center resonance frequency, λ_p, reported on the x axis of the graph. The resulting curves show a smooth resonance-like behavior, indicating that all the metamaterials have a similar reflectance and transmittance spectrum [see also the study of Aljunid *et al.* (*24*)]. For a more quantitative analysis, we perform an FDFD simulation of the metamaterials. We extract the expected far-field reflectance and transmittance intensities of the metamaterials. The FDFD results are in good quantitative agreement with the experimental data. However, we perform a global adjustment of the contrast of the reflectance and transmittance of the FDFD results by a factor of 0.7 and 0.5, respectively. This adjustment accounts for frequency-independent optical losses, which are not encountered in the FDFD simulation. Contributions may come from photon scattering at the metamaterials, imperfect size matching of the beam to the metamaterial, or possible long-range inhomogeneity of the metamaterial geometry.

We now tune the laser onto the $F = 4 \leftrightarrow F' = 5$ hyperfine transition scanning over a frequency range of 100 MHz = ~20Γ, where Γ = 5.2 MHz is the bare frequency width of the atomic transition. The demodulated signals at 9 MHz of the beam reflectance correspond to the red points on Fig. 3. We observe a strong modification of the Doppler-free spectrum due to the presence of the metamaterials with respect to a plain dielectric window (see blue points on Fig. 3). The hyperfine structure of the D2 line is spectrally resolved with our SR experiment, because the frequency spacing between hyperfine components (200 MHz between $F' = 3$ and $F' = 4$ and 250 MHz between $F' = 4$ and $F' = 5$) are much larger than the width of the observed spectra (~10 to 20 MHz). Also, the plasmonic resonance is much broader than the hyperfine splitting; therefore, its effects are identical on all hyperfine components.

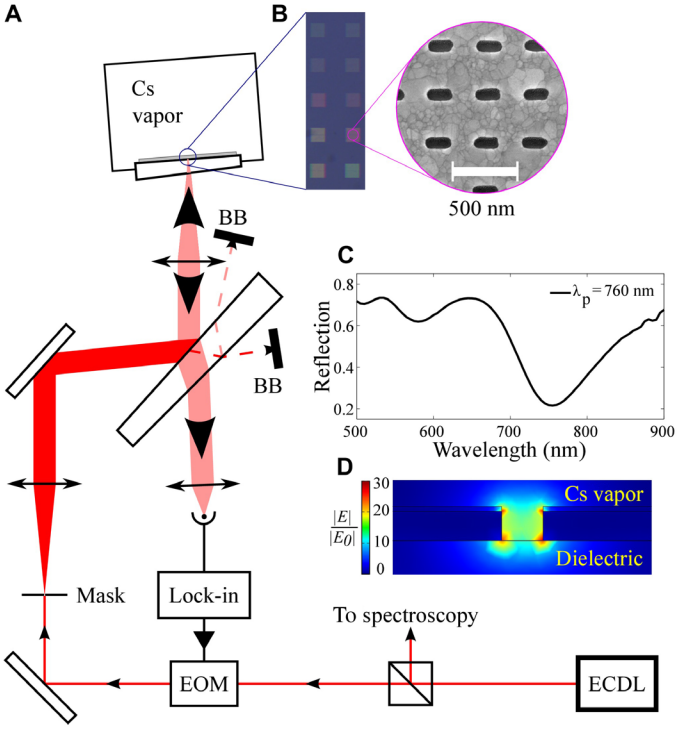

Fig. 1. Schematic of the experimental setup. (**A**) Experimental setup. (**B**) Real-color back-illuminated images of the 10 metamaterials. The zoom corresponds to a scanning electron microscope image. (**C**) Typical reflectance curve of a metamaterial showing a main plasmon resonance at λ = 760 nm. (**D**) Cut along one nanoslit. The false colors represent the electric field magnitude, normalized by the amplitude of the incident field, as obtained by a finite-difference frequency-domain (FDFD) simulation. EOM, electro-optic modulator; BB, beam block.

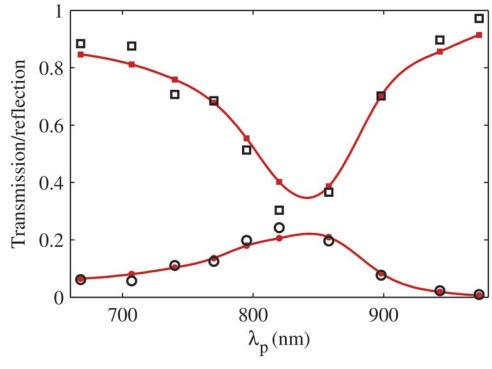

Fig. 2. Optical characterization of the metamaterials. Experimental reflection (open squares) and transmission (open circles) of the 10 metamaterials measured with the 852-nm laser. The x axis corresponds to λ_p, the position of the plasmon resonance of each metamaterial. The solid red squares (circles) correspond to the reflection (transmission) obtained by an FDFD numerical simulation. The lines, connecting FDFD results, are guides to the eye.

Similar SR spectra can be obtained for the $F = 4 \leftrightarrow F' = 3$ and 4 transitions, albeit with a smaller amplitude due to weaker transition probabilities.

To further analyze the experimental data, we model the metamaterial by a spatially homogeneous bulk material having the same thickness and far-field reflectance/transmittance at normal incidence. This mean-field approximation holds for the thermal vapor at the vicinity of the metamaterial because the large spatial variation of the plasmon (see example in Fig. 1D) is well smoothed by the finite response time of the atomic coherence (see the Supplementary Materials for more details).

In SR spectroscopy with a homogeneous material interface, the vapor can be characterized by an effective electric susceptibility, χ. Its frequency derivative is given, in the Doppler limit ($k\,\bar{u} \gg \Gamma$), by (*25*)

$$\frac{d\chi(\omega)}{d\omega} = \frac{2Nk\mu^2}{\sqrt{\pi}\,\bar{u}\,\epsilon_o\hbar}\int_0^\infty dz \int_0^\infty dz' \frac{(z-z')e^{ik(z+z')}}{\mathcal{L}_o(\omega,z) - \mathcal{L}_o(\omega,z')} \quad (1)$$

$\mathcal{L}_o(\omega,z) = \frac{\Gamma}{2} - i(\omega - \omega_o + \frac{\Delta C_3 z^{-3}}{2})$ is the Lorentzian line shape of the bare atomic resonance, corrected by the z^{-3} Casimir-Polder frequency shift in the nonretarded regime. Here, ω_o is the bare atomic resonance, k is the wave number of the laser beam, and μ is the two-level atomic dipole moment. Spectroscopic experiments are sensitive to the energy difference between levels. We therefore denote ΔC_3 the difference of van der Waals coefficients between lower and upper states. In our analysis, ΔC_3 is considered to be complex. As can be seen from the equations above, its real and imaginary parts denote a distance-dependent shift and linewidth respectively. The metamaterial/vapor interface is located at $z = 0$. We note that the phase factor, $e^{ik(z+z')}$, rapidly averages the effective susceptibility to zero for $z, z' \gg k^{-1}$. As an important consequence, only the atoms located in a layer of thickness k^{-1} contribute to the SR signal. Moreover, as can be seen in Eq. 1 and already discussed above, the signal is Doppler-free. We note as well that, because $\chi \ll 1$, the index of refraction of the atomic vapor reads as $n = 1 + \chi/2$. Under this approximation, the complex reflection coefficient of the electric field for the dielectric/metamaterial/vapor system can be linearized as

$$r = r_o + \rho\chi \quad (2)$$

where r_o and ρ depend only on the indices of refraction of the metamaterial n' and of the dielectric substrate n_d (see Materials and Methods). In the Doppler limit, $\chi(\omega)$ is obtained by integration of Eq. 1. In the weak-modulation limit, that is, $\beta \ll 1$, we find that the demodulated signal has the following expression for the in-phase signal (*25*)

$$V_p(\omega) = V_0 Re\{r_0^*\rho[\chi(\omega+\omega_m) - \chi(\omega-\omega_m)]\} \quad (3)$$

and for the in-quadrature signal

$$V_q(\omega) = V_0 Im\{r_0^*\rho[\chi(\omega+\omega_m) + \chi(\omega-\omega_m) - 2\chi(\omega)]\} \quad (4)$$

V_0 is a factor of proportionality. Within the mean-field approximation, the complex factor $r_0^*\rho$ can be evaluated analytically (see Materials and Methods for more details). It depends on n', n_d, and the metamaterial thickness. By mixing the real and imaginary parts of the susceptibility, the factor $r_0^*\rho$ gives the main contribution of the modification of the atomic resonance line shape induced by the plasmon resonance observed in Fig. 3. Also, the product of the susceptibility with the complex value $r_0^*\rho$ in Eqs. 3 and 4 leads to a Fano-like resonance of the atoms/metamaterial hybrid system as shown by some of us in the study of Aljunid *et al.* (*24*) and by Stern and coauthors using a Kretschmann geometry (*23*). In addition to the Fano-like resonance, the Casimir-Polder interaction induces an additional contribution to the SR signal that we are now aiming to reveal and discuss.

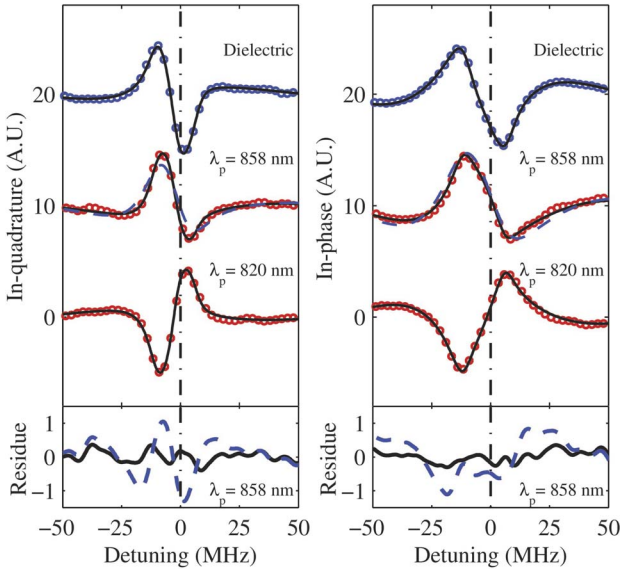

Fig. 3. SR spectra. In-phase and in-quadrature SR spectra of the plain windows (blue dots at top curves) and of two metamaterials (red dots). More spectra are shown in the Supplementary Materials. The black solid curves are the fits using Eq. 1. The dashed blue line is a fit assuming $\mathrm{Im}[\Delta C_3] = 0$ for the metamaterial at $\lambda_p = 858$ nm. The residues correspond to the metamaterial at $\lambda_p = 858$ nm. The units are the same as for the main top curves. A.U., arbitrary units.

Using Eqs. 1 to 4, we perform a fit of the SR signals for the different metamaterials including the bare dielectric substrate. The fitting parameters are the atomic resonance linewidth Γ, the complex value of ΔC_3, and a common V_0 value. The effective index of refraction of the metamaterial n', thus the factor $r_0^*\rho$, is extracted from the FDFD simulation (*29*, *30*). The results of the fitting procedure correspond to the black curves in Fig. 3. We observed an agreement with the experimental data. The volume atomic resonance width (away from the surface) is found to be $\Gamma = 10(3)$ MHz, that is, slightly larger than the bare linewidth of 5.2 MHz. This increase of the linewidth, encountered as well on the dielectric interface, has been also reported in similar studies (*3*). It can be due to residual collisional broadening. An imaginary part for the ΔC_3 has to be considered. To illustrate this point, we perform another fit, setting $\mathrm{Im}[\Delta C_3] = 0$. Under this constraint, we observe that the convergence of the fitting procedure is not satisfactory (see residue comparison in Fig. 3 for $\lambda_p = 858$ nm).

The complex van der Waals coefficients obtained from the fits are shown in Fig. 4 (A and B). The real part of the ΔC_3 coefficient (Fig. 4A) displays a dispersive type of resonant behavior centered at $\lambda_p \sim 840$ nm. At the blue side of the resonance, we observe a significant increase of the interaction, with respect to its off-resonant value ~5 kHz μm^3, followed by a sharp decrease that leads to a nearly vanishing value of the interaction at the red side of the resonance. The resonance width is in agreement with the plasmon linewidth of 60 nm, confirming the plasmonic origin of the modification of the ΔC_3 values. The presence and evolution of the imaginary (dissipative) part for the van der Waals coefficients, shown in Fig. 4B, corresponds to a decrease of the atomic lifetime

associated with enhancement of the vacuum mode density at the plasmonic resonance. This enhanced emission rate can be also be understood as an increase of the Purcell factor as observed, for example, with ultracold gas (*31*) or nanoantennas (*32*). The enhanced radiation emission of the atom/metamaterial system can finally either be coupled to electromagnetic propagating modes or be lost because of ohmic losses in the metal. The SR technique does not distinguish between those two cases.

DISCUSSION

We compare our experimental measurements with the QED theory of atom-surface interactions. A complete analysis of the resonant Casimir-Polder interaction depends on the knowledge of the dielectric properties of the metamaterial for both real and imaginary frequencies. For this purpose, we fit the dielectric constant ε, extracted by FDFD simulations, to an analytical model that accounts for the resonances of the metamaterial as well as the surface plasmon resonance of silver itself. We then calculate the difference of the Casimir-Polder frequency shift between $Cs(6P_{3/2})$ and $Cs(6S_{1/2})$, which is the experimentally measured quantity in SR spectroscopy. Here, we take into account both nonresonant and resonant components. The nonresonant term does not depend on the position of the plasmon resonance and is mostly governed by the metallic response over the entire frequency spectrum (*33*, *34*). The influence of the plasmon resonance is contained in the resonant contribution (*34*, *35*), which is only relevant for the excited-state $Cs(6P_{3/2})$ interaction potential. It concerns the resonant photons on the $6S_{1/2}\leftrightarrow 6P_{3/2}$ transition, and it is mainly at the origin of the observed Casimir-Polder resonant behavior (see the Supplementary Materials). The results of the nonretarded model are shown as dashed lines in Fig. 4 (C and D). The theoretical predictions exhibit a resonant behavior similar to the experimental findings, showing that our model captures the essence of the physical mechanism behind the tuning of the atom-surface interaction. However, the amplitude of the resonance is smaller than the experimentally measured one.

In our experiments, the plasmonic resonances coincide with the probing SR wavelength. This suggests that we are not in a pure near-field regime and that retardation effects cannot be neglected (*36*). In the retarded regime, the dephasing of the oscillating dipole with respect to its image causes the resonant term of the excited state to oscillate with a period of λ/2 (atomic transition wavelength) (*33*, *34*). The phase and amplitude of these oscillations depend on the surface reflection coefficient (*36*), which varies significantly with the plasmonic resonance of the metamaterial. For this reason, retardation can affect the amplitude and the shape of the ΔC_3 resonance (see also the Supplementary Materials). To strengthen our analysis further, we calculate an "effective" van der Waals coefficient as a function of distance, defined as $C_3(z) = \frac{\delta E(z) z^3}{\hbar} + i\frac{\delta\Gamma(z) z^3}{2\hbar}$, where $\delta E(z)$ is the Casimir-Polder shift and $\delta\Gamma(z)/2$ the linewidth of a given atomic level. We find that they both deviate significantly from the near field (van der Waals approximation) even at nanometric distances away from the metamaterial surface. Analysis of the SR line shapes reveals that the relevant distance range is 70 to 100 nm, in agreement with a characteristic probing depth ~λ/2π. In Fig. 4 (C and D), we compare our experimental results with the real and imaginary parts of an effective $\Delta C_3(z)$ coefficient for distances between 70 and 100 nm, where $\Delta C_3(z)$ is the difference between the effective van der Waals coefficients of excited $(6P_{3/2})$ and ground states $(6S_{1/2})$. Retardation effects enhance the amplitude of the ΔC_3 resonance but fail to exactly reproduce the experimental data. It should be noted that our calculations were performed for a semi-infinite effective bulk material. However, considering a finite layer of 50 nm has a minor impact on the ΔC_3 values (see the Supplementary Materials for more details). We also mention that the real and imaginary parts of the ΔC_3 coefficient in the case of pure silver are ~4.5 and ~0.5 kHz μm^3, respectively. This is in agreement with the experimentally measured off-resonant values of the coefficient, confirming the validity of our data analysis. We finally note that in our mean field analysis, we have considered a homogeneous metamaterial characterized by one effective dielectric constant. A future more detailed analysis would have to take the anisotropy of the metamaterial into consideration. For this purpose, the theoretical framework for anisotropic interactions described by Gorza *et al.* (*22*) has to be expanded to include the effects of retardation.

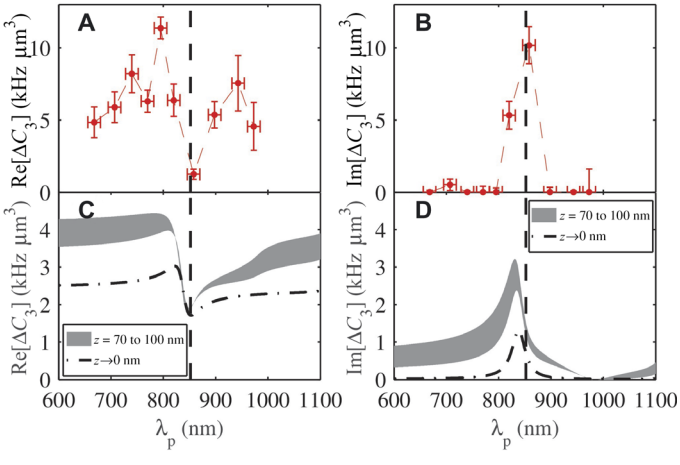

Fig. 4. The van der Waals coefficient. ΔC_3 coefficients as a function of λ_p, the position of the plasmon resonance. Real part (**A**) and imaginary part (**B**) extracted from the fits of the SR signals. (**C**) and (**D**) are the real and imaginary parts of the C_3 coefficients computed from the model. The dot-dashed curve corresponds to the nonretarded case ($z\rightarrow 0$). The retarded contribution is taken into account by considering an effective distance ranging from 70 to 100 nm. It corresponds to the shaded gray surface. The vertical dashed lines indicate the position of the atomic resonance.

To conclude, we use planar metamaterials as a test bed to control the Casimir-Polder frequency shift of the D2 line of Cs atoms. When the plasmon resonance almost coincides with the atomic resonance, the Casimir-Polder frequency shift nearly vanishes. Across the different metamaterials, the Casimir-Polder interaction is characterized by the usual real coefficient leading to a dispersive resonance, as well as a nonzero on-resonance dissipative response.

Finally, we mention that gratings have been previously used in Casimir (*37*, *38*) and nonresonant Casimir-Polder experiments with Bose-condensed ground-state Rb atoms (*39*). In these cases, the experiments have strenuously tested various theoretical models/approximations for calculating vacuum forces with nontrivial surface geometries, demonstrating the nonadditivity of the Casimir-Polder interaction at short distances. Our measurements are different because we explore resonant Casimir-Polder interactions with excited-state atoms next to a silver metamaterial. It might be interesting to note that our results show that nanopatterning the silver surface, typically removing 7% of the material, can in some cases increase the Casimir-Polder interaction by more than 100% with respect to pure silver. This is a powerful illustration of Casimir-Polder nonadditivity. Our theoretical analysis, based on the mean-field approximation, reproduces the main characteristics of the Casimir-Polder resonance albeit with a smaller amplitude. It would be worth comparing our experimental results with numerical models that fully account for the shape of the metamaterial.

MATERIALS AND METHODS

Sample fabrication

Our experiments were conducted in a vacuum chamber with metamaterial samples fabricated on one of the optical access windows of the chamber (*24*). A 3° quartz wedge window was used to support a 50-nm layer of silver deposited by thermal evaporation and protected by an 8-nm layer of SiO_2. The metamaterials were then fabricated by focused ion beam milling. Each metamaterial array was 200 μm × 200 μm in size. We also fabricated a window in the silver film for reference measurements. The chamber base pressure was 10^{-8} mbar, whereas the cesium vapor pressure was maintained at a temperature of 80°C corresponding to a vapor pressure of $P = 10^{-4}$ mbar.

Derivation of the $r_0^*\rho$ parameter

The reflection coefficient in the mean-field approximation is given by (*40*)

$$r = \frac{(n_d - n')(n' + n) + (n_d + n')(n' - n)e^{\frac{2in'l\omega}{c}}}{(n_d - n')(n' + n) - (n_d + n')(n' - n)e^{\frac{2in'l\omega}{c}}} \quad (5)$$

where n_d, n', and n are, respectively, the index of refraction of the dielectric substrate, of the effective bulk material (describing the metamaterial), and of the atomic vapor. l is the effective bulk material thickness. The index of refraction of the atomic vapor is given by $n = 1 + \chi/2$, where χ is the atomic susceptibility. Because $\rho = \frac{\partial r}{\partial \chi}\big|_{\chi=0}$, the complex coefficient $r_0^*\rho$ is found to be

$$r_0^*\rho = \frac{4|r_o|^2 n_d n'^2 e^{\frac{2in'l\omega}{c}}}{(1+n')^2(n'^2 - n_d^2) + 2(1-n'^2)(n_d^2 + n'^2)e^{\frac{2in'l\omega}{c}} + (1+n')^2(n'^2 - n_d^2)e^{\frac{4in'l\omega}{c}}} \quad (6)$$

Calculation of the Casimir-Polder interaction

Here, we calculated the Casimir-Polder interaction between an excited-state atom and a metameterial using the perturbation approach first described by Wylie and Sipe (*33*, *34*), also followed in numerous other works. In the framework of the mean-field approximation, metamaterials were considered uniform and isotropic materials with an effective dielectric constant extracted by FDFD simulations for a wavelength range between 500 and 1500 nm. Casimir-Polder calculations rely on the knowledge of the dielectric function at the entire frequency range, and for this purpose, we fitted the FDFD data using the following analytic function

$$\epsilon(\omega) = 1 - \frac{\omega_p^2}{\omega^2 + i\,\gamma_p\omega} + \sum_j \frac{f_j\omega_j^2}{(\omega_j^2 - \omega^2) - i\gamma_j\omega} \quad (7)$$

The first part of the equation is a Drude model that accounts for the bulk properties of silver. The plasmon frequency ω_p and dissipation γ_p are common for all metamaterials. The second part models the metamaterial resonances. The amplitude (f_j), frequency (ω_j), and dissipation (γ_j) of each resonance are smoothly varying functions of the plasmonic resonance (λ_p) of the metamaterial. By interpolating these parameters, we can calculate the Casimir-Polder interaction for a continuous range of metamaterials (see Fig. 4, C and D). We stress in this study that our calculation does not critically depend on the analytic model used to fit the dielectric constant. This is because the physics is mostly contained on the resonant part of the interaction that depends on $\mathrm{Re}[\frac{\epsilon(\omega_o)-1}{\epsilon(\omega_o)+1}]$, where ω_o is the atomic resonance frequency. At zero temperature ($T = 0$), the ground-state potential as a function of distance z writes

$$\delta E(z) = -\frac{1}{\pi}\sum_n \omega_{gn}\mu_\alpha^{gn}\mu_\beta^{ng}\int_0^\infty d\xi \frac{G_{\alpha\beta}(z, i\xi)}{\xi^2 + \omega_{gn}^2} \quad (8)$$

The excited-state potential is as follows

$$\delta E(z) = -\frac{1}{\pi}\sum_n \omega_{en}\mu_\alpha^{en}\mu_\beta^{ne}\int_0^\infty d\xi \frac{G_{\alpha\beta}(z; i\xi)}{\xi^2 + \omega_{en}^2} - \sum_n \mu_\alpha^{gn}\mu_\beta^{ng} Re\left[G_{\alpha\beta}(\vec{r}_o\vec{r}_o|\omega_{en}|)\right]\left(1 - \Theta(\omega_{en})\right) \quad (9)$$

whereas the distance-dependent atomic-level linewidth is given by

$$\delta\Gamma(z) = 2\sum_n \mu_\alpha^{gn}\mu_\beta^{ng} Im\left[G_{\alpha\beta}(\vec{r}_o\vec{r}_o|\omega_{en}|)\right]\left(1 - \Theta(\omega_{en})\right) \quad (10)$$

Here, the summation has to be made on all possible dipole couplings terms. The transition frequencies ω_{gn} and ω_{en} are considered positive for upward couplings and negative for downward couplings. $\Theta(\omega_{en})$ is the Heaviside function, ξ is an integration variable, μ_α^{gn}, μ_β^{ng}, μ_α^{en}, and μ_β^{ne} are the dipole moment matrix elements, and $G_{\alpha\beta}(z, i\xi)$ is the linear susceptibility function defined by Wylie and Sipe (*33*, *34*) and by Laliotis and Ducloy (*36*). We used the Einstein notation, implying a summation over the index variables α and β that denoted the Cartesian coordinate components. In the near field, the linear susceptibility is a diagonal matrix whose elements are proportional to $\frac{1}{(2z)^3}\frac{\varepsilon(\omega)-1}{\varepsilon(\omega)+1}$.

SUPPLEMENTARY MATERIALS

Supplementary material for this article is available at http://advances.sciencemag.org/cgi/content/full/4/2/eaao4223/DC1

Stationary surface plasmon waves
Mean-field approximation for the atomic vapor response
Experimental data and fit of SR signal for all metamaterials
Resonant photon contribution to the Casimir-Polder interaction
Retardation effects on SR
Finite thickness of the metamaterial
fig. S1. Electric field simulations.
fig. S2. SR spectra.
fig. S3. Resonant contribution to the Casimir-Polder interaction.
fig. S4. Retardation effects on SR.
fig. S5. Finite thickness of the metamaterial.

REFERENCES AND NOTES

1. H. B. G. Casimir, D. Polder, The influence of retardation on the London-van der Waals forces. *Phys. Rev.* **73**, 360–372 (1948).
2. M. Oria, M. Chevrollier, D. Bloch, M. Fichet, M. Ducloy, Spectral observation of surface-induced van der Waals attraction on atomic vapour. *EPL (Europhys. Lett.)* **14**, 527–532 (1991).
3. M. Chevrollier, M. Fichet, M. Oria, G. Rahmat, D. Bloch, M. Ducloy, High resolution selective reflection spectroscopy as a probe of long-range surface interaction : Measurement of the surface van der Waals attraction exerted on excited Cs atoms. *J. Phys. II* **2**, 631–657 (1992).
4. M. Fichet, G. Dutier, A. Yarovitsky, P. Todorov, I. Hamdi, I. Maurin, S. Saltiel, D. Sarkisyan, M.-P. Gorza, D. Bloch, M. Ducloy, Exploring the van der Waals atom-surface attraction in the nanometric range. *EPL (Europhys. Lett.)* **77**, 54001 (2007).

5. V. Sandoghdar, C. I. Sukenik, E. A. Hinds, S. Haroche, Direct measurement of the van der Waals interaction between an atom and its images in a micron-sized cavity. *Phys. Rev. Lett.* **68**, 3432–3435 (1992).
6. C. I. Sukenik, M. G. Boshier, D. Cho, V. Sandoghdar, E. A. Hinds, Measurement of the Casimir-Polder force. *Phys. Rev. Lett.* **70**, 560–563 (1993).
7. A. Landragin, J.-Y. Courtois, G. Labeyrie, N. Vansteenkiste, C. I. Westbrook, A. Aspect, Measurement of the van der Waals Force in an Atomic Mirror. *Phys. Rev. Lett.* **77**, 1464–1467 (1996).
8. H. Bender, P. W. Courteille, C. Marzok, C. Zimmermann, S. Slama, Direct measurement of intermediate-range Casimir-Polder potentials. *Phys. Rev. Lett.* **104**, 083201 (2010).
9. J. M. Obrecht, R. J. Wild, M. Antezza, L. P. Pitaevskii, S. Stringari, E. A. Cornell, Measurement of the temperature dependence of the Casimir-Polder force. *Phys. Rev. Lett.* **98**, 063201 (2007).
10. D. J. Alton, N. P. Stern, T. Aoki, H. Lee, E. Ostby, K. J. Vahala, H. J. Kimble, Strong interactions of single atoms and photons near a dielectric boundary. *Nat. Phys.* **7**, 159–165 (2011).
11. M. Gullans, T. G. Tiecke, D. E. Chang, J. Feist, J. D. Thompson, J. I. Cirac, P. Zoller, M. D. Lukin, Nanoplasmonic lattices for ultracold atoms. *Phys. Rev. Lett.* **109**, 235309 (2012).
12. A. Goban, C. L. Hung, J. D. Hood, S. P. Yu, J. A. Muniz, O. Painter, H. J. Kimble, Superradiance for Atoms Trapped along a Photonic Crystal Waveguide. *Phys. Rev. Lett.* **115**, 063601 (2015).
13. E. Vetsch, D. Reitz, G. Sagué, R. Schmidt, S. T. Dawkins, A. Rauschenbeutel, Optical interface created by laser-cooled atoms trapped in the evanescent field surrounding an optical nanofiber. *Phys. Rev. Lett.* **104**, 203603 (2010).
14. S. Okaba, T. Takano, F. Benabid, T. Bradley, L. Vincetti, Z. Maizelis, V. Yampol'skii, F. Nori, H. Katori, Lamb-Dicke spectroscopy of atoms in a hollow-core photonic crystal fibre. *Nat. Commun.* **5**, 4096 (2014).
15. J. D. Thompson, T. G. Tiecke, N. P. de Leon, J. Feist, A. V. Akimov, M. Gullans, A. S. Zibrov, V. Vuletić, M. D. Lukin, Coupling a single trapped atom to a nanoscale optical cavity. *Science* **340**, 1202–1205 (2013).
16. D. E. Chang, K. Sinha, J. M. Taylor, H. J. Kimble, Trapping atoms using nanoscale quantum vacuum forces. *Nat. Commun.* **5**, 4343 (2014).
17. A. Goban, C.-L. Hung, S.-P. Yu, J. D. Hood, J. A. Muniz, J. H. Lee, M. J. Martin, A. C. McClung, K. S. Choi, D. E. Chang, O. Painter, H. J. Kimble, Atom–light interactions in photonic crystals. *Nat. Commun.* **5**, 3808 (2014).
18. S.-P. Yu, J. D. Hood, J. A. Muniz, M. J. Martin, R. Norte, C.-L. Hung, S. M. Meenehan, J. D. Cohen, O. Painter, H. J. Kimble, Nanowire photonic crystal waveguides for single-atom trapping and strong light-matter interactions. *Appl. Phys. Lett.* **104**, 111103 (2014).
19. H. Failache, S. Saltiel, M. Fichet, D. Bloch, M. Ducloy, Resonant van der Waals repulsion between excited Cs atoms and sapphire surface. *Phys. Rev. Lett.* **83**, 5467–5470 (1999).
20. H. Failache, S. Saltiel, M. Fichet, D. Bloch, M. Ducloy, Resonant coupling in the van der Waals interaction between an excited alkali atom and a dielectric surface: An experimental study via stepwise selective reflection spectroscopy. *Eur. Phys. J. D* **23**, 237–255 (2003).
21. A. Laliotis, T. Passerat de Silans, I. Maurin, M. Ducloy, D. Bloch, Casimir–Polder interactions in the presence of thermally excited surface modes. *Nat. Commun.* **5**, 4364 (2014).
22. M.-P. Gorza, S. Saltiel, H. Failache, M. Ducloy, Quantum theory of van der Waals interactions between excited atoms and birefringent dielectric surfaces. *Eur. Phys. J. D* **15**, 113–126 (2001).
23. L. Stern, M. Grajower, U. Levy, Fano resonances and all-optical switching in a resonantly coupled plasmonic–atomic system. *Nat. Commun.* **5**, 4865 (2014).
24. S. A. Aljunid, E. A. Chan, G. Adamo, M. Ducloy, D. Wilkowski, N. I. Zheludev, Atomic response in the near-field of Nanostructured Plasmonic Metamaterial. *Nano Lett.* **16**, 3137–3141 (2016).
25. M. Ducloy, M. Fichet, General theory of frequency modulated selective reflection. Influence of atom surface interactions. *J. Phys. II* **1**, 1429–1446 (1991).
26. H. Failache, S. Saltiel, A. Fischer, D. Bloch, M. Ducloy, Resonant quenching of gas-phase Cs atoms induced by surface polaritons. *Phys. Rev. Lett.* **88**, 243603 (2002).
27. J. P. Woerdman, M. F. H. Schuurmans, Spectral narrowing of selective reflection from sodium vapour. *Opt. Commun.* **14**, 248–251 (1975).
28. A. M. Akul'shin, V. L. Velichanskii, A. S. Zibrov, V. V. Nikitin, V. V. Sautenkov, E. K. Yurkin, N. V. Senkov, Collisional broadening of intra-Doppler resonances of selective reflection on the D_2 line of cesium. *JETP Lett.* **36**, 303–307 (1982).
29. X. Chen, T. M. Grzegorczyk, B.-I. Wu, J. Pacheco Jr., J. A. Kong, Robust method to retrieve the constitutive effective parameters of metamaterials. *Phys. Rev. E Stat. Nonlin. Soft Matter Phys.* **70**, 01608 (2004).
30. J. Baker-Jarvis, E. J. Vanzura, W. A. Kissick, Improved technique for determining complex permittivity with the transmission/reflection method. *IEEE Trans. Microw. Theory Tech.* **38**, 1096–1103 (1990).
31. C. Stehle, C. Zimmermann, S. Slama, Cooperative coupling of ultracold atoms and surface plasmons. *Nat. Phys.* **10**, 937–942 (2014).
32. G. M. Akselrod, C. Argyropoulos, T. B. Hoang, C. Ciracì, C. Fang, J. Huang, D. R. Smith, M. H. Mikkelsen, Probing the mechanisms of large Purcell enhancement in plasmonic nanoantennas. *Nat. Photonics* **8**, 835–840 (2014).
33. J. M. Wylie, J. E. Sipe, Quantum electrodynamics near an interface. *Phys. Rev. A* **30**, 1185–1193 (1984).
34. J. M. Wylie, J. E. Sipe, Quantum electrodynamics near an interface. II. *Phys. Rev. A* **32**, 2030–2043 (1985).
35. M. Fichet, F. Schuller, D. Bloch, M. Ducloy, van der Waals interactions between excited-state atoms and dispersive dielectric surfaces. *Phys. Rev. A* **51**, 1553–1564 (1995).
36. A. Laliotis, M. Ducloy, Casimir-Polder effect with thermally excited surfaces. *Phys. Rev. A* **91**, 052506 (2015).
37. F. Intravaia, S. Koev, I. W. Jung, A. A. Talin, P. S. Davids, R. S. Decca, V. A. Aksyuk, D. A. R. Dalvit, D. López, Strong Casimir force reduction through metallic surface nanostructuring. *Nat. Commun.* **4**, 2515 (2013).
38. H. B. Chan, Y. Bao, J. Zou, R. A. Cirelli, F. Klemens, W. M. Mansfield, C. S. Pai, Measurement of the Casimir force between a gold sphere and a silicon surface with nanoscale trench arrays. *Phys. Rev. Lett.* **101**, 030401 (2008).
39. H. Bender, C. Stehle, C. Zimmermann, S. Slama, J. Fiedler, S. Scheel, S. Y. Buhmann, V. N. Marachevsky, Probing atom-surface interactions by diffraction of Bose-Einstein condensates. *Phys. Rev. X* **4**, 011029 (2014).
40. M. Chevrollier, M. Oriá, J. G. de Souza, D. Bloch, M. Fichet, M. Ducloy, Selective reflection spectroscopy of a resonant vapor at the interface with a metallic layer. *Phys. Rev. E Stat. Nonlin. Soft Matter Phys.* **63**, 046610 (2001).

Acknowledgments: A.L. thanks the UMI Majulab and the Centre for Quantum Technologies for supporting his trip to Singapore. We wish to thank N. I. Zheludev and E. Lassalle for fruitful discussions. **Funding:** This work was supported by the Singapore Ministry of Education Academic Research Fund Tier (grant no. MOE2011-T3-1-005). **Author contributions:** E.A.C. and S.A.A. performed the SR spectroscopy measurements. G.A. designed and fabricated the metamaterial. E.A.C., S.A.A., A.L., M.D., and D.W. conducted the data analysis. A.L., M.D., and D.W. established the theoretical model and the physical interpretations. D.W. coordinated the project and is responsible for all the materials disclosed in the paper and/or the Supplementary Materials. All authors participated in the writing of the manuscript. **Competing interests:** The authors declare that they have no competing interests. **Data and materials availability:** All data needed to evaluate the conclusions in the paper are present in the paper and/or the Supplementary Materials. Additional data related to this paper may be requested from the authors.

Submitted 18 July 2017
Accepted 5 January 2018
Published 2 February 2018
10.1126/sciadv.aao4223

Citation: E. A. Chan, S. A. Aljunid, G. Adamo, A. Laliotis, M. Ducloy, D. Wilkowski, Tailoring optical metamaterials to tune the atom-surface Casimir-Polder interaction. *Sci. Adv.* **4**, eaao4223 (2018).